


Article

Optimization of the Process Parameters of an Air-Screen Cleaning System for Frozen Corn Based on the Response Surface Method

Ning Zhang ^{1,2}, Jun Fu ^{1,2,3,*} , Zhi Chen ^{2,3}, Xuegeng Chen ⁴ and Luquan Ren ^{1,2}

¹ Key Laboratory of Bionic Engineering, Ministry of Education, Jilin University, Changchun 130022, China; nzhang19@mails.jlu.edu.cn (N.Z.); lqren@jlu.edu.cn (L.R.)

² College of Biological and Agricultural Engineering, Jilin University, Changchun 130022, China; chenzhi@caamm.org.cn

³ Chinese Academy of Agricultural Mechanization Sciences, Beijing 100083, China

⁴ College of Mechanical and Electrical Engineering, Shihezi University, Shihezi 832000, China; chenxg431@163.com

* Correspondence: fu_jun@jlu.edu.cn

Abstract: The threshing of frozen corn is accompanied by breakage and adherence, which influence the cleaning performance when the corn-cleaning mixture is separated and cleaned. In order to reduce the impurity ratio and loss ratio during frozen corn cleaning and provide theoretical support for frozen corn combine harvesting, this study employed a self-made air-screen cleaning system with adjustable parameters. The optimal process parameters of frozen corn cleaning were determined by using the response surface method (RSM). The influences of the fan speed (FS), vibrational frequency (VF), and screen opening (SO) on the cleaning performance were explored. The results showed that all three process parameters had significant effects on the impurity ratio (IR) and loss ratio (LR). The fan speed had the most significant impact. The cleaning performance was optimal when the fan speed was 102.7 rad/s, the vibration frequency was 6.42 Hz, and the screen opening was 21.9 mm, corresponding to a 0.80% impurity ratio and a 0.61% loss ratio. The predicted values of the regression models were consistent with the experimental results with a relative error of less than 5%. The reliability and accuracy of regression models were established and confirmed.

Keywords: frozen corn; freeze adhesion; corn combine harvester; cleaning performance; parameter optimization



Citation: Zhang, N.; Fu, J.; Chen, Z.; Chen, X.; Ren, L. Optimization of the Process Parameters of an Air-Screen Cleaning System for Frozen Corn Based on the Response Surface Method. *Agriculture* **2021**, *11*, 794. <https://doi.org/10.3390/agriculture11080794>

Academic Editor: José Pérez-Alonso

Received: 1 August 2021

Accepted: 18 August 2021

Published: 19 August 2021

Publisher's Note: MDPI stays neutral with regard to jurisdictional claims in published maps and institutional affiliations.



Copyright: © 2021 by the authors. Licensee MDPI, Basel, Switzerland. This article is an open access article distributed under the terms and conditions of the Creative Commons Attribution (CC BY) license (<https://creativecommons.org/licenses/by/4.0/>).

1. Introduction

Corn is the most widely produced crop in the world, and it is an important food and feed source. Corn production has great significance in ensuring food security [1–4]. In Canada, Ukraine, and northeast China, owing to high latitudes, the temperature is already below zero when corn is harvested. In particular, owing to the long harvesting period, a large amount of corn is harvested after frost and snowfall [5]. The physical properties of corn change after freezing, which results in a high loss ratio in the combine harvesting operation. The combine harvester can simultaneously complete the processes of ear picking, threshing, cleaning, and collection, resulting in high operational efficiency and low operating costs [6]. Therefore, it is widely used for frozen corn and harvesting of other grains.

In combine harvesting, cleaning is an important procedure. The performance of the cleaning system in a combine harvester directly affects the loss ratio and the impurity ratio [7]. In order to improve the performance of the cleaning system, several researchers have carried out numerous analyses on cleaning system in harvesters. Li et al. [8] simulated and analyzed the motion of rice particles in cleaning device utilizing the discrete element method (DEM) coupled with computational fluid dynamics (CFD). Their simulation results

revealed that the longitudinal velocity of the short straw was significantly affected by inlet airflow velocity. Badretdinov et al. [9] established a kinematic model of the linkage structure of a grain combine harvester cleaning system by deriving coordinates, velocity, and acceleration of the nodal points. For wind speed distribution, Ueka et al. [10] analyzed the turbulent flow characteristics of the cleaning airflow. The results found that the main factors affecting the airflow distribution were the friction and pressure change of material particles. Gebrehiwot et al. [11] simulated and compared the airflow distributions of three forward curved centrifugal fans. The results indicated that adding a cross-flow opening in the width direction of the centrifugal fan outlet could enhance the utilization efficiency of airflow. To investigate cleaning screen types, Wang et al. [12,13] designed several corn cleaning screens, such as a curved screen, combined screen, and rubber screen. Sabashkin et al. [14] proposed a cylinder screen with a screw dispenser for grain cleaning. Ivanov et al. [15] established a mathematical model of grain movement in cylindrical screen, and discussed the impact of feed rate and rotation speed on grain screening. Krzysiak et al. [16] invented a new conical rotary screen and investigated the effect of the drum inclination angle on cleaning performance. To address the blocking problem of the cleaning screen, Cheng et al. [17] proposed an accumulation rule for the corn cob blockage mass in a chaff screen as the operating hours increased. The response surface method (RSM) was used to obtain the optimal vibration parameters with minimal corn cob blockage. For the real-time monitoring of loss during the cleaning process, Xu et al. [18] developed a sieve loss sensor based on the signal analysis of impacts. In addition, Craessaerts et al. [19,20] proposed a multivariate input selection methodology and a fuzzy control system. By selecting and controlling the variables of the sieve, the cleaning performance of the combine harvester was optimized under different operation conditions. In general, all of these studies were conducted under conditions in which the temperature was above zero at the time of grain harvesting.

However, the physical properties of corn change after freezing, and some corn kernels adhere to each other, which introduce challenges to the cleaning process. Unfortunately, no experimental studies of air-screen cleaning systems have been reported for such conditions, and to date, no optimal process parameters have been specified. Therefore, the objective of this study is to optimize the process parameters of the air-screen cleaning system for frozen corn to reduce the impurity ratio (IR) and loss ratio (LR). The characteristic dimensions and the physical properties of components in the cleaning mixture were measured. A single-factor design and the Box–Behnken design (BBD) were implemented. The effects of the fan speed (FS), vibrational frequency (VF), the screen opening (SO) on cleaning performance were analyzed, respectively. The experiments were conducted to determine the combination of process parameters to obtain the optimal IR and LR. Using the impurity ratio and loss ratio as response values, the optimal combination of process parameters was determined and verified by experiments. The results may have potential to use for setting frozen corn combine harvesting parameters.

2. Materials and Methods

In this section, we provide a brief introduction of the materials used for the cleaning study. Then, we describe the experimental apparatus. Next, we present the experimental designs, including the single-factor and the Box–Behnken experimental designs. Finally, we present the method used to analyze experimental data.

2.1. Materials

For the cleaning study on frozen corn, a corn-cleaning mixture was prepared. The corn cultivar Feitian 358 was selected as the sample. First, corn ears with the husks were picked by hand in Changchun city (N 43°56′, E 125°14′), Jilin province. The picking time was from 10 to 15 December 2020, while the corn ears were frozen. Then, the ears were threshed on a longitudinal axial threshing cylinder test device [5]. Referring to the operating parameters of corn grain harvesters in Northeast China, the feed rate of corn ears was 8.5 kg/s, the

drum speed was 40.3 rad/s, and the concave clearance was 40 mm [5]. The corn-cleaning mixture was collected and stored outdoors. The mass of all preparative mixture was 3135 kg. Finally, a corn cleaning test was performed. The whole experimental process, from threshing to cleaning, was completed outdoors within 7 days after picking the corn ears. Over the experimental periods, the outdoor average temperature ranged from -10.2 to -12.6 °C. This means that the experimental materials were in a native frozen state throughout the experimental periods.

2.2. Experimental Apparatus

The air-screen cleaning system used in this study is shown in Figure 1. The air-screen cleaning system separates corn kernels from impurities under the action of airflow and vibration. It mainly consists of frame, feeding hopper, oscillating plate, fan, fan drive motor, crank, crank drive motor, swing, upper screen, upper screen box, lower screen, lower screen box, tailing screen, and collection box. The upper screen and tailing screen are bolted onto the upper screen box. Similarly, the lower screen is bolted onto the lower screen box. In Figure 1, the nearside plate of the lower screen box is hidden so as to observe the position of the lower screen. The oscillating plate, upper screen box, and lower screen box were powered for reciprocation with a 7.5 kW electric motor through the crank and swing. A FR500-4T-7.5G frequency converter (Freon Electric Co., Ltd., Shenzhen, China) was used to adjust the vibrational frequency of the oscillating plate, upper screen box, and lower screen box in a range from 0 to 25 Hz. The fan was driven by a 2.2 kW electric motor and was adjusted by a FR150-2S-2.2B frequency converter (Freon Electric Co., Ltd., Shenzhen, China), the speed of which ranged from 0 to 150.7 rad/s. All screens were chaffer sieves with adjustable opening. The screen slices of the chaffer sieve were arranged in parallel. The vertical distance between two adjacent parallel screen slices is the screen opening (SO).

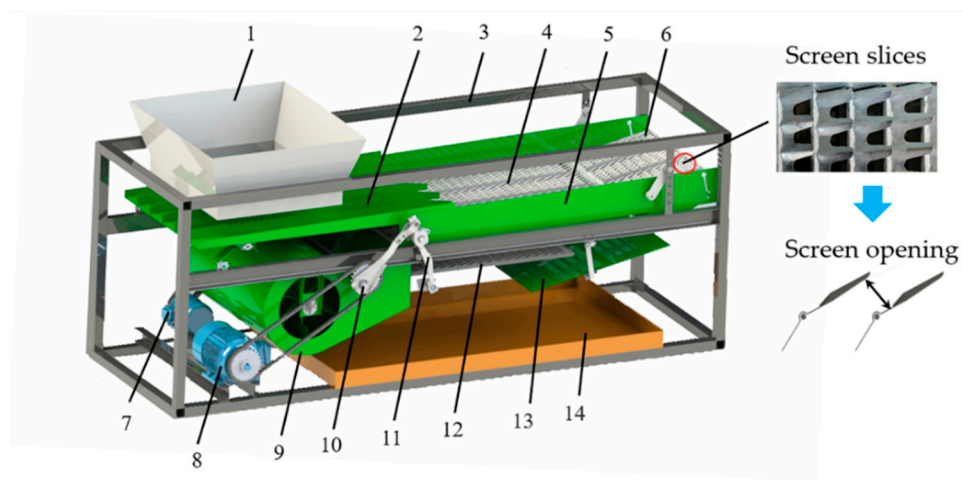


Figure 1. Air-screen cleaning system: 1. feeding hopper, 2. oscillating plate, 3. frame, 4. upper screen, 5. upper screen box, 6. tailing screen, 7. fan drive motor, 8. crank drive motor, 9. fan, 10. crank, 11. swing, 12. lower screen, 13. lower screen box, and 14. collection hopper.

2.3. Experimental Design

2.3.1. Single-Factor Experiment

According to the material properties and the operating principle of the air-screen cleaning system, the impurity ratio (IR) and loss ratio (LR) depend on several factors, such as fan speed (FS), vibration frequency (VF), and screen opening (SO) [21]. A single-factor experiment was designed to analyze the effects of these three factors [22,23]. The single-factor experiment was arranged with six values for each factor with the feed rate of the corn-cleaning mixture set to 5.5 kg/s. For each set of parameters, a single trial was repeated three times. The experimental scheme is shown in Table 1. Given that air flow plays an important role in the cleaning process, the fan outlet airflows at different fan speeds were

measured with an AS866 hot-film anemometer (SMART SENSOR, Hong Kong, China) and the airflows corresponding to the six fan speed values were 7.9, 9.4, 10.8, 12.7, 14.3, and 16.8 m/s.

Table 1. Experimental scheme design of the single-factor experiment.

Numbers	Factors	Values	Condition
1–5	Fan speed (FS) (rad/s)	73.2, 83.7, 94.2, 104.7, 115.2, 125.6	VF = 5 Hz SO = 22 mm
6–10	Vibration frequency (VF) (Hz)	3, 4, 5, 6, 7, 8	FS = 104.7 rad/s SO = 22 mm
11–15	Screen opening (SO) (mm)	18, 20, 22, 24, 26, 28	FS = 104.7 rad/s VF = 5 Hz

2.3.2. Box–Behnken Experiment

A Box–Behnken design (BBD) with three factors and three levels was implemented to explore the interaction between factors [24,25]. The coded levels are shown in Table 2. The impurity ratio and loss ratio were used as evaluation indexes. As shown in Table 3, the experiment was performed with seventeen groups of trials including twelve combinations of factors and five replicates at the center point [26]. The feed rate of the corn-cleaning mixture was set to 5.5 kg/s.

Table 2. Levels of each experimental factor.

Levels	Fan Speed (rad/s)	Vibration Frequency (Hz)	Screen Opening (mm)
−1	94.2	5	20
0	104.7	6	22
1	115.2	7	24

Table 3. The experimental design and results.

Numbers	Factors			Evaluation Indexes	
	Fan Speed (rad/s)	Vibration Frequency (Hz)	Screen Opening (mm)	Impurity Ratio (%)	Loss Ratio (%)
1	−1	−1	0	1.39	0.69
2	1	−1	0	0.85	1.47
3	−1	1	0	0.94	0.71
4	1	1	0	0.79	1.24
5	−1	0	−1	1.05	0.64
6	1	0	−1	0.9	1.65
7	−1	0	1	1.32	0.82
8	1	0	1	1.03	1.19
9	0	−1	−1	0.99	1.03
10	0	1	−1	0.89	1.01
11	0	−1	1	1.25	1.08
12	0	1	1	0.9	0.82
13	0	0	0	0.73	0.73
14	0	0	0	0.85	0.66
15	0	0	0	0.83	0.69
16	0	0	0	0.75	0.73
17	0	0	0	0.87	0.74

After cleaning, the mixture was collected in the collection box, and the impurities therein were manually selected and weighed to calculate the impurity ratio. All discharged materials at the end of the tailing screen were gathered in a net bag, and the corn kernels therein were picked out and weighed to calculate the loss ratio. The impurity ratio and loss ratio were calculated by using the following equations [7]:

$$IR = \frac{m_i}{m_h} \times 100\%, \quad (1)$$

$$LR = \frac{m_l}{m_t} \times 100\%, \quad (2)$$

where m_i is the mass in kg of impurities in the collection box, m_h is the mass in kg of corn kernels in the collection box, m_l is the mass in kg of lost kernels, and m_t is the total mass in kg of the corn-cleaning mixture.

2.4. Data Analysis Method

In this study, the experimental results of the BBD were statistically analyzed using Design-Expert 2021 software (Stat-Ease Inc., Minneapolis, MN, USA). The response surface method (RSM) was applied to analyze the experimental data. Quadratic regression models were evaluated through the coefficient of determination (R^2) [27]. The significance of each factor for the experimental evaluation indexes was determined using the analysis of variance (ANOVA) [27], and the significance level was $p = 0.05$. Subsequently, response surface plots for interactions were generated using RSM. In addition, the optimal values of process parameters and the predicted IR and LR values were determined. The optimal parameters obtained from the regression analysis were further verified by experiments.

3. Results

In this section, the physical properties of materials are described, and the effects of process parameters on the cleaning performance are analyzed. Regression models and the optimal parameters combination are presented.

3.1. Physical Properties of Components

The physical properties of materials are an important basis for the design and determination of parameters for an air-screen cleaning system. After freezing, the physical properties of corn components change, which affects the cleaning performance [28]. Therefore, in order to provide a data reference, the physical properties of each component in the corn-cleaning mixture were measured. The corn-cleaning mixture included five crop components, namely, corn kernels, corn cobs, corn stalks, corn husks, and corn stigma, together with the noncrop component, ice. Five hundred grams corn kernels, 100 g corn cobs, 50 g corn stalks and 50 g corn husks were randomly selected from the mixture as a group of samples to determine the moisture contents. Samples were prepared in triplicate and were dried in a DZF-6050 thermostatic drying oven (Rongshida Electric Equipment Co., Ltd., Kunshan, China) at 105 ± 1 °C for 24 h [29]. The moisture contents of kernels, cobs, stalks, hulks, and stigma, measured on a wet basis method, were $24.8 \pm 0.19\%$, $54.5 \pm 0.22\%$, $68.3 \pm 0.15\%$, $26.6 \pm 0.17\%$, and $25.7 \pm 0.11\%$, respectively.

The shapes of corn kernels were horse-toothed, conical, and spherical [30]. Taking the horse-toothed kernel as an example, the characteristic dimensions comprise the upper width (W_1), bottom width (W_2), height (H_h), and thickness (T). The dimensions were measured by a digital caliper with 0.01 mm accuracy (Prokits Industries Co., Ltd., Shanghai, China). The characteristic dimensions of corn kernel in three shapes are shown in Table 4.

Table 4. Shapes and characteristic dimensions of corn kernels in three shapes.

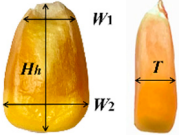
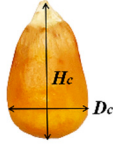
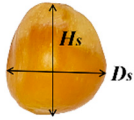
Shape	Characteristic Dimensions	Value	Proportion (%)
 Horse-toothed kernel	W_1 (mm)	4.44–6.39	88.2
	W_2 (mm)	7.32–9.61	
	H_h (mm)	10.18–14.20	
	T (mm)	4.01–6.46	

Table 4. Cont.

Shape	Characteristic Dimensions	Value	Proportion (%)
 Conical kernel	D_c (mm)	4.65–6.23	7.5
	H_c (mm)	9.26–13.65	
 Spherical kernel	D_s (mm)	3.98–6.27	4.3
	H_s (mm)	3.65–6.51	

The length (L_c), radius (R_c), and broken angle (α) were determined as the characteristic dimensions of corn cobs. The length (L_s) and radius (R_s) were determined as the characteristic dimensions of corn stalks. The dimensions were measured with the digital caliper and an angle gauge with 0.01° accuracy (Dongmei Instruments Ltd., Shenzhen, China). The characteristic sizes and the measurement results are listed in Tables 5 and 6.

Table 5. Characteristic dimensions of corn cobs.

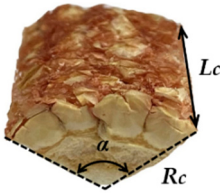

	Characteristic Dimensions	Value	Proportion (%)
 Corn cob	R_c (mm)	10–20	38.1
		20–30	36.4
		30–40	15.4
		40–50	5.5
		50–60	2.7
		60–70	1.9
	L_c (mm)	8–10	22.2
		10–12	37.8
		12–14	26.4
		14–16	4.5
	α ($^\circ$)	0–90	51.2
		90–180	29.0
		180–270	9.1
		270–360	10.7

Table 6. Characteristic dimensions of corn stalks.

	Characteristic Dimensions	Value	Proportion (%)
 Corn stalk	L_s (mm)	10–20	11.9
		20–30	38.5
		30–40	31.7
		40–50	12.8
		50–60	5.1
	R_s (mm)	5–6	6.9
		6–7	44.2
		7–8	35.7
		8–9	13.2

The coefficient of static friction was measured by applying a self-made test platform (Figure 2). A corn kernel was placed on the wall; the slope was then lifted by adjusting the screw and was stopped just as the kernel began to slide [31]. The angle displayed on the digital protractor was recorded. When the coefficient of friction between kernels

was measured, a corn kernel was placed on the wall that was glued with kernels, and then the previous step was repeated. The coefficient of static friction can be calculated by Equation (3):

$$\mu = \tan \theta \quad (3)$$

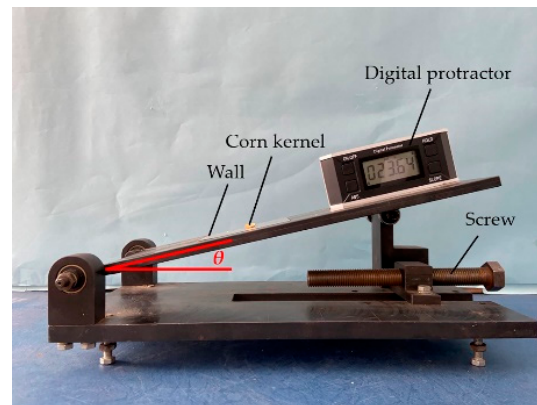


Figure 2. Platform to test the static friction coefficient.

The coefficient of rolling friction was measured by using the slope method [32]. As shown in Figure 3, a corn stalk was released at no initial velocity at the top of the slope and rolled on the horizontal surface until static. The vertical distance h and rolling distance d were measured, and coefficient of rolling friction was calculated using Equation (4):

$$f = \frac{h}{d} \quad (4)$$

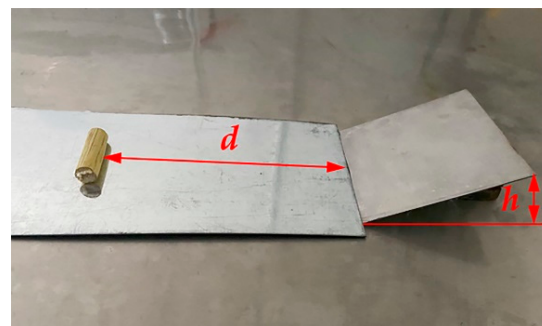


Figure 3. Platform to test the roll friction coefficient.

The coefficient of restitution was measured by the self-made restitution coefficient test platform (Figure 4). We used a dropping test to determine the coefficient of restitution between each component and screen [33]. A corn kernel was released from the position of height H_0 and collided with the horizontal collision plane. A high-speed camera was used to record the rebound height of the kernel H_1 after the collision. The coefficient of restitution can be calculated by using Equation (5). We used a pendulum test to determine the coefficient of restitution between components [34]. As shown in Figure 4, two corn kernels were glued and connected with fishing line. The kernel on the right was released at the height H_0 with no initial velocity and collided with another kernel. After collision, kernels reached the heights H_1 and H_2 . The coefficient of restitution was calculated by using Equation (6). The results of the physical properties characterizing the contact are shown in Table 7.

$$e_w = \sqrt{\frac{H_1}{H_0}} \quad (5)$$

$$e_p = \frac{\sqrt{H_2} - \sqrt{H_1}}{\sqrt{H_0}} \quad (6)$$

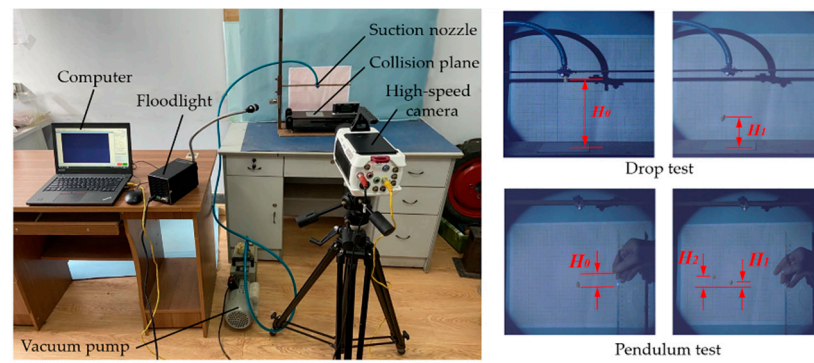


Figure 4. Platform to test the restitution coefficient.

Table 7. The physical properties of characterizing contact between components.

Property	Coefficient of Restitution	Coefficient of Static Friction	Coefficient of Rolling Friction
Corn kernel–corn kernel	0.37	0.36	0.04
Corn kernel–corn cob	0.28	0.62	0.02
Corn kernel–corn stalk	0.26	0.34	0.05
Corn kernel–screen	0.58	0.39	0.05
Corn cob–corn cob	0.25	0.78	0.02
Corn cob–corn stalk	0.24	0.39	0.04
Corn cob–screen	0.35	0.65	0.02
Corn stalk–corn stalk	0.23	0.38	0.06
Corn stalk–screen	0.30	0.34	0.05

When corn was harvested in the frozen state, some corn kernels after threshing presented the phenomenon of freeze-adhesion, as shown in Figure 5. Adhering kernels had difficulty penetrating the screen due to the overall increase in dimensions. Therefore, the characteristic dimensions of adhering kernels were measured, as shown in Table 8.



Figure 5. Adhering kernels and their characteristic dimensions.

Table 8. Types and characteristic dimensions of adhesive kernels.

Types	A (mm)	B (mm)	H (mm)
Two-kernel adhesion	6.9–8.8	7.3–9.6	12.2–14.5
Three-kernel adhesion	11.9–14.3	7.5–10.1	12.0–15.4
Four-kernel adhesion	15.5–17.2	7.2–10.5	11.8–15.9

3.2. Results of Single-Factor Experiment

3.2.1. Fan Speed

The nonlinear fitting curve in Figure 6 indicates the influence of fan speed on the impurity ratio and loss ratio. With the increase in fan speed, the IR decreased from 1.45% to 0.86%. Conversely, the LR increased from 0.75% to 1.42%. It can be seen in Figure 6 that the reduction in IR was more significant, ranging from 73.2 to 104.7 rad/s. The IR maintained a small decline from 104.7 to 125.6 rad/s. The LR increased slightly at first and then experienced a sharp increase when the fan speed exceeded 104.7 rad/s. As the fan speed increased, more impurities, such as corn cobs and husks, were blown out from the cleaning system, resulting in a decrease in the IR. However, the blowing effect of airflow on corn kernels was strengthened with the increase in the fan speed. Some kernels intermingled within impurities were blown out without being screened, which caused a large loss.

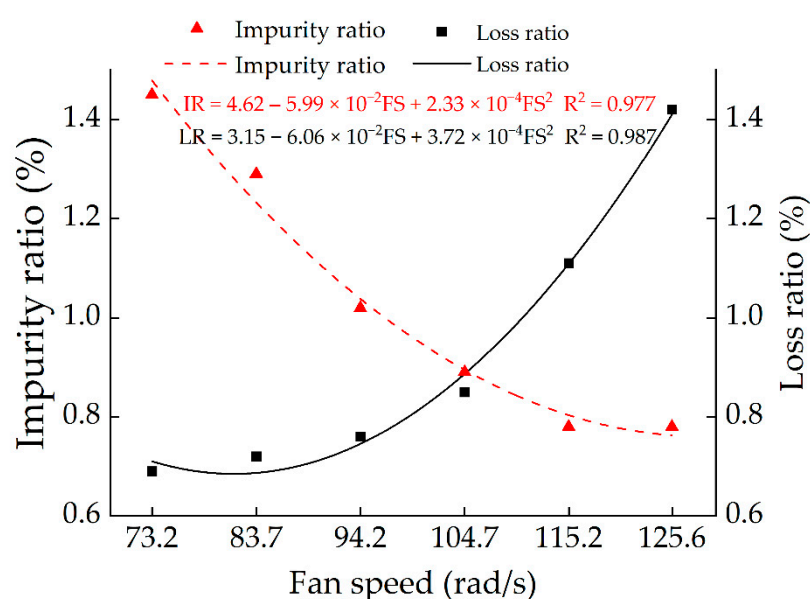


Figure 6. Influence of fan speed on the impurity ratio and loss ratio.

3.2.2. Vibration Frequency

The nonlinear fitting curve in Figure 7 indicates the influence of vibration frequency on the impurity ratio and loss ratio. With the increase in the vibration frequency, the IR decreased from 1.44% to 0.80%. Conversely, the LR increased from 0.79% to 1.18%. In particular, the IR decreased mainly in the range of 3–6 Hz, and it leveled off within the range of 6–8 Hz. The rising tendency of the LR caused by the vibration frequency was similar to that caused by the fan speed. The LR increased significantly when the vibration frequency exceeded 6 Hz. The increase in vibration frequency facilitated layering and dispersal of material from the cleaning mixture on the screen surface, which was conducive to kernel penetration. The airflow on the screen surface was evenly distributed, which facilitated the backward movement of impurities. Therefore, the IR continuously decreased. However, the kernel loss increased as the vibration frequency increased. The reason for this is that the screening time of the cleaning-mixture decreased as the vibration frequency increased. Some corn kernels were discharged from the chaff screen before passing through it.

3.2.3. Screen Opening

The nonlinear fitting curve in Figure 8 indicates the influence of the screen opening on the impurity ratio and the loss ratio. With the increase of the screen opening, the LR decreased from 1.39% to 0.72%. Conversely, the IR increased from 0.73% to 1.42%. It can be seen that the IR increased slightly at first. After reaching 22 mm, the rise in the IR became steep. The LR showed a sharp downward trend from 18 to 24 mm and a slow downward

trend from 24 to 28 mm. As the screen opening increased, corn kernels were more likely to pass through the screen rather than exit the cleaning system, explaining the decline in the LR. With a small screen opening, a large number of corn stalks and corn cobs were unable to penetrate the screen due to the size limitation. When the size of the screen opening increased until it exceeded that of impurities, the impurities passed through the screen and entered the collection box, which caused an increase in the IR.

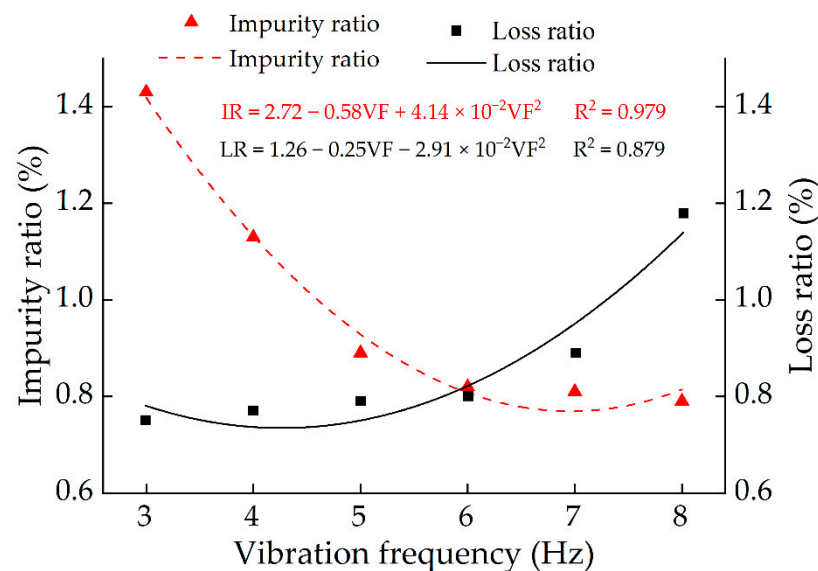


Figure 7. Influence of vibration frequency on the impurity ratio and loss ratio.

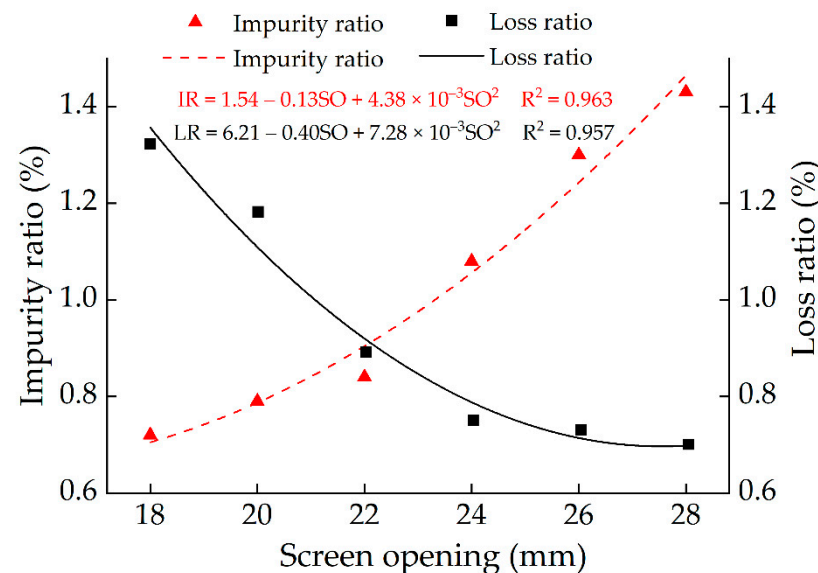


Figure 8. The influence of screen opening on the impurity ratio and the loss ratio.

3.3. Analysis of Variance

The results of ANOVA on the impurity ratio are shown in Table 9. In the ANOVA results, a p -value of less than 0.05 indicates that the model term had a significant influence. The p -value of this model was less than 0.001, which indicates that the regression model of the IR was significant. For the linear terms, the results clearly show that FS, VF, and SO all had a significant influence on the IR. Moreover, FS was the most significant factor, with an F-value of 43.15, and VF was the second most significant. For the interaction terms, only FS–VF had a significant influence on the IR. Moreover, the quadratic terms (FS)² and (SO)²

also had a significant influence on the IR. Therefore, after excluding nonsignificant terms, the regression model of the IR is shown as follows:

$$IR = 31.834 - 0.274FS - 1.119VF - 1.158SO + 9.286 \times 10^{-3}FS \times VF + 1.152 \times 10^{-3}(FS)^2 + 3.5500 \times 10^{-2}(SO)^2 \quad (7)$$

Table 9. ANOVA of the impurity ratio.

Cause of Variance	Sum of Squares	Freedom	Mean Square	F-Value	p-Value	Significant
Model	0.57	9	0.064	17.25	0.0006	*
FS	0.16	1	0.16	43.15	0.0003	*
VF	0.12	1	0.12	31.14	0.0008	*
SO	0.056	1	0.056	15.17	0.0059	*
FS–VF	0.038	1	0.038	10.28	0.0149	*
FS–SO	0.0049	1	0.0059	1.32	0.2876	
VF–SO	0.016	1	0.016	4.22	0.0789	
(FS) ²	0.068	1	0.068	18.36	0.0036	*
(VF) ²	0.015	1	0.015	4.03	0.0847	
(SO) ²	0.085	1	0.085	22.95	0.0020	*
Residual	0.026	7	0.003699			
Lack of Fit	0.010	3	0.003458	0.89	0.5186	
Pure Error	0.016	4	0.003.88			
Total	0.60	16				

* Significant ($p < 0.05$).

The results of ANOVA on the loss ratio are shown in Table 10. The p -value of this model was less than 0.0001, implying that the regression model of the LR was extremely significant. For the linear terms, it was clear that FS, VF, and SO all had a significant influence on changing the LR. Moreover, FS was the most significant factor. Furthermore, the F-value of FS far outweighed that of VF and SO. For the interaction terms, only FS–VF had a significant influence on changing the LR. Moreover, the quadratic terms of (FS)², (VF)², and (SO)² had a significant influence on changing the LR. Therefore, the regression model of the LR after excluding the nonsignificant items is shown as follows:

$$LR = 34.508 - 0.317FS - 2.787VF - 0.935SO + 6.429 \times 10^{-3}FS \times VF + 1.73 \times 10^{-3}(FS)^2 + 0.176(VF)^2 + 2.594 \times 10^{-2}(SO)^2 \quad (8)$$

Table 10. ANOVA for the loss ratio.

Cause of Variance	Sum of Squares	Freedom	Mean Square	F-Value	p-Value	Significant
Model	1.69	9	0.19	58.86	<0.0001	*
FS	1.24	1	1.24	388.90	<0.0001	*
VF	0.023	1	0.023	7.25	0.0310	*
SO	0.034	1	0.034	10.60	0.0140	*
FS–VF	0.018	1	0.018	5.71	0.0481	*
FS–SO	0.0081	1	0.0081	2.54	0.1550	
VF–SO	0.0004	1	0.0004	0.031	0.8645	
(FS) ²	0.15	1	0.15	48.29	0.0002	*
(VF) ²	0.13	1	0.13	41.01	0.0004	*
(SO) ²	0.045	1	0.045	14.21	0.0070	*
Residual	0.022	7	0.003189	58.86		
Lack of Fit	0.018	3	0.005908		0.0739	
Pure Error	0.0046	4	0.00115			
Total	1.71	16				

* Significant ($p < 0.05$).

3.4. Response Surface Analysis

The response surface plots shown in Figure 9 depict the effects of interactions between FS, VF, and SO on the IR. The IR presents a similar trend in Figure 9a–c; it first decreases

and then increases with the increase in FS, VF, and SO. However, comparing the curve gradient of the response surface shows that the changing trend shown in Figure 9a is the strongest. The p -value of FS–VF listed in Table 9 is greater than those of FS–SO and VF–SO. Therefore, the interaction of FS–VF for the IR had the most significant effect on the IR.

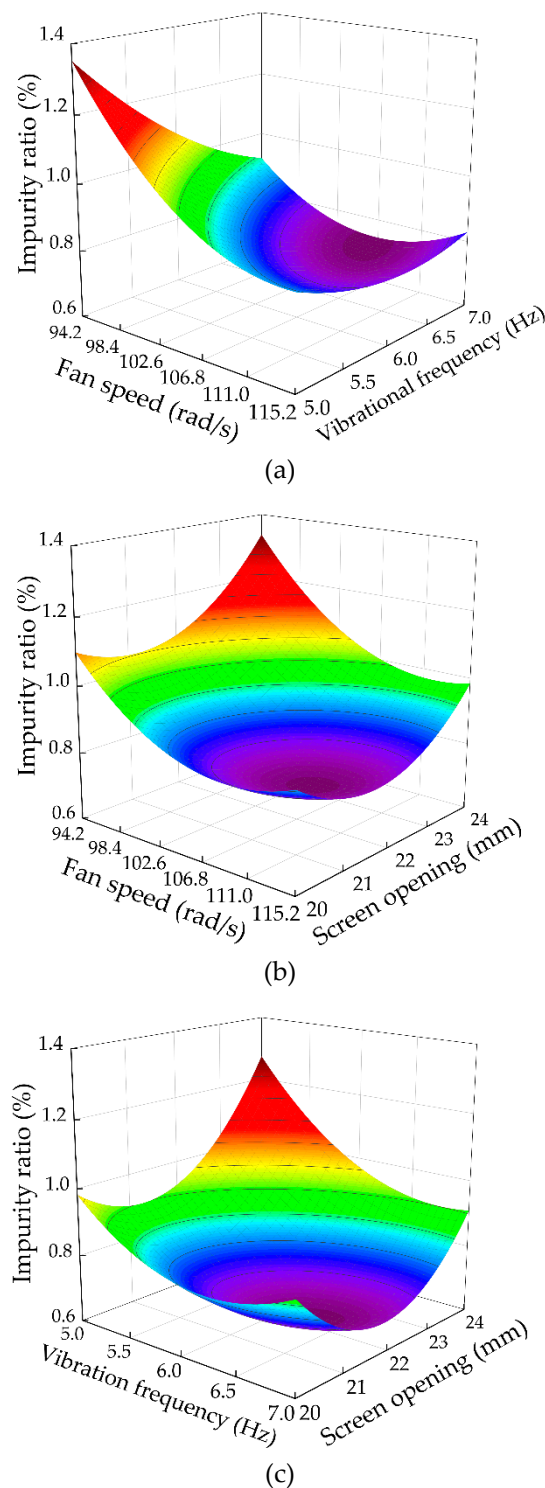


Figure 9. Response surface plots for interaction between the pairs (a) FS–VF, (b) FS–SO, and (c) VF–SO.

The response surface plots shown in Figure 10 depict the effects of interactions between FS, VF, and SO on the LR. In the cleaning process, the LR significantly increased with the

increase in FS. The enhancement of the LR can be explained by the stronger carrying effect of the airflow on the corn kernels. The increase in VF led to a corresponding decline in the LR when the VF was low. However, a further increase in VF resulted in a rise of the LR. The trend of the LR caused by the increase of SO was similar to that of VF. Comparing the curve gradient of the response surfaces in Figure 10 and the p -values in Table 10 confirms that the interaction of FS–VF had the most significant effect on the LR.

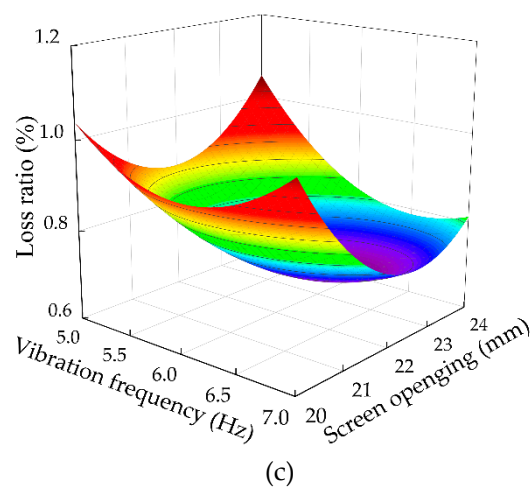
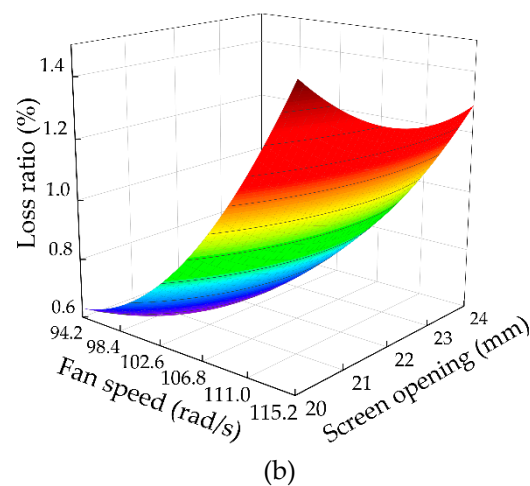
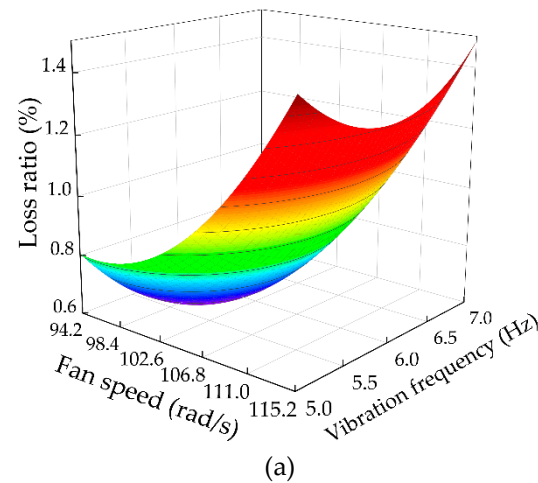


Figure 10. Response surface plots for interaction between the pairs (a) FS–VF, (b) FS–SO, and (c) VF–SO.

3.5. Optimization and Verification

The analysis above shows that the IR and the LR varied inversely with the variation in process parameters. Response surface optimization [35,36] was carried out. The aim of optimization was to obtain the optimal combination of FS, VF, and SO to simultaneously minimize the IR and LR in the process of frozen corn cleaning. Therefore, the response values of the IR and LR were taken as the minimum values. The ranges of FS, VF, and SO were constrained to 94.2–115.2 rad/s, 5–7 Hz, and 20–24 mm, respectively. The optimal combination was obtained using Design-Expert 2021 software. The IR and LR were both minimized when the FS was 102.7 rad/s, the VF was 6.42 Hz, the SO was 21.9 mm. The predicted values of IR and LR were 0.80% and 0.61%, respectively. Three validation experiments were then carried out under the optimal parameters. As shown in Table 11, the experimental results were highly consistent with the predicted values, with a relative error of less than 5%. These results indicate that the optimization model is reliable in the frozen corn cleaning operation.

Table 11. Results of validation experiments and predicted values.

	1	2	3	Mean	Prediction	Relative Error (%)
IR (%)	0.74	0.82	0.76	0.77	0.80	3.89
LR (%)	0.59	0.66	0.68	0.64	0.61	4.69

4. Discussion

4.1. Physical Properties

When frozen corn is harvested, the ice contained in the mixture causes the phenomenon of corn freeze-adhesion. According to statistical data, adhering kernels accounted for 1% of the corn-cleaning mixture. Amongst them, there were 74% cases with two-kernel adhesion, 24% cases with three-kernel adhesion, and 2% with four-kernel adhesion. Some physical properties of components were determined, including characteristic dimensions, coefficient of restitution, coefficient of static friction, and coefficient of rolling friction. Compared with literature reports [13,30,31], no notable differences in characteristic dimensions of nonadhesive corn kernels, corn cobs and corn stalks were observed. However, the proportion of corn cobs decreased by 1.2% because in the frozen state, corn cobs are difficult to break when corn ears are threshed. Most corn cobs with full or half lengths were discharged at the end of the threshing drum and did not enter the cleaning system. The coefficient of restitution, coefficient of static friction, and coefficient of rolling friction of frozen corn were slightly higher than those of nonfrozen corn, which is similar to the results reported in the literature [33].

4.2. Single-Factor Experiment

With the increase in the fan speed, the impurity ratio continuously decreased while the loss ratio continuously increased. When the fan speed was 73.2 rad/s, the minimum loss ratio occurred, which was 0.69%; however, the maximum impurity ratio of 1.45% was observed. When the fan speed was 125.6 rad/s, the impurity ratio of 0.78% was the lowest, while the loss ratio peaked at 1.42%. For cleaning performance, both the low impurity ratio and loss ratio should be taken into account. Therefore, as presented in Figure 6, the fan speed interval 94.2–115.2 rad/s was superior, ensuring both a lower impurity ratio and loss ratio. Similarly, as shown in Figures 7 and 8, the superior interval of vibration frequency and screen opening were 5–7 Hz and 20–24 mm, respectively. The results of the single-factor experiment provided the data support that selected the levels of each experimental factor in the Box–Behnken experiment.

4.3. Response Surface Analysis

The ANOVA results for response surface demonstrated that fan speed was the most important factor for affecting both the impurity ratio and loss ratio. The response surface plots also showed that the change of impurity ratio with fan speed (Figure 9a,b)

was stronger than those with vibrational frequency (Figure 9a,c) and screen opening (Figure 9b,c). This changing tendency was the same for the loss ratio. For the interaction terms, the function was realized by synergism between FS and VF, which led to a decrease in impurity ratio and an increase in loss ratio. The optimal combination was fan speed 102.7 rad/s, vibration frequency 6.42 Hz, and screen opening 21.9 mm. Correspondingly, the impurity ratio was 0.80% and loss ratio was 0.61%. Results of validation tests were a 0.77% impurity ratio and a 0.64% loss ratio, which meet the requirements of Chinese National Standard GB/T 21962-2020 for the impurity ratio and loss ratio in corn combine harvesters ($IR \leq 2\%$, $LR \leq 2\%$).

4.4. Cleaning Process Parameters between Frozen and Nonfrozen Corn

At present, no studies have reported on cleaning process parameters for frozen corn. In contrast to harvesting at above-zero temperature, there were certain differences in the parameter values. In literature reports [12,13,35], the values of fan speed covered a range from 78.5 to 94.2 rad/s, and the values of vibrational frequency covered a range from 4.45 to 6 Hz. In this study, the optimal values of the fan speed and vibration frequency were 102.7 rad/s and 6.42 Hz, which were higher than optimum values for harvesting above zero. This is because of the physical properties of crop components and ice in the mixture. Firstly, the increase of static friction coefficient reduced the moving velocity of the mixture. Secondly, as the screen slices of chaffer screen were inclined upwards, this caused rebound forward of mixture to occur frequently when the screen was in reciprocating movement. The increase of coefficient of restitution enabled the backward motion velocity of the mixture increase, but it also meant that the forward rebound velocity of the mixture was increased. Thus, these physical properties affected the movement of the mixture. Thirdly, frozen kernel adhesion weakened the fluidity of the mixture as small pieces of ice were present. In particular, this effect was exacerbated by ice attaching to the oscillating plate and screen surface. Hence, the fan speed and vibrational frequency needed to be larger to promote the flow of the mixture. Additionally, there was not much difference in screen opening values.

5. Conclusions

In this study, the process parameters of an air-screen cleaning system for frozen corn were optimized by using the response surface method (RSM). The physical properties of materials were measured. The influences of fan speed, vibration frequency, and screen opening on evaluation indexes were analyzed. The single-factor experiment results indicate that the impurity ratio was negatively correlated with fan speed and vibration frequency, and it was positively correlated with screen opening. The loss ratio was positively correlated with fan speed and vibration frequency, and it was negatively correlated with screen opening. The optimal combination of process parameters was a fan speed of 102.7 rad/s, vibrational frequency of 6.42 Hz, and screen opening of 21.9 mm. Under this condition, the impurity ratio was 0.80% and the loss ratio was 0.61%. Compared to the results of validation experiments, the relative error of the predicted values was less than 5%, proving the reliability of the regression models that were determined. This study provided a theoretical basis for the process of optimizing air-screen cleaning systems for frozen corn.

It is worth noting that this study has some limitations. First, the influence of the variation in moisture content was not explored. The moisture content influences the physical properties of corn and then affects the parameter ranges. Second, in the study, we only investigated the cleaning of a single corn cultivar. The differences between corn varieties in frozen state merit further study.

Therefore, further research is needed to address these limitations. The effect of moisture content as a factor on cleaning performance will be investigated. Additional corn varieties require consideration. More types of screen and hole sizes in the screen will be selected. Based on the test results, a new cleaning system will be designed to improve higher cleaning performance for frozen corn harvesting.

Author Contributions: Conceptualization, J.F.; methodology, J.F.; validation, N.Z.; investigation, N.Z.; resources, J.F.; writing—original draft preparation, N.Z.; writing—review and editing, J.F.; supervision, Z.C., X.C., and L.R.; project administration, J.F.; funding acquisition, J.F. All authors have read and agreed to the published version of the manuscript.

Funding: This research was funded by the International Science and Technology Cooperation Project of Science and Technology Development Program of Jilin Province, grant number 20190701055GH.

Institutional Review Board Statement: Not applicable.

Informed Consent Statement: Not applicable.

Data Availability Statement: Not applicable.

Acknowledgments: The authors are grateful for the frozen corn provided by the Experimental Base of Agriculture of Jilin University.

Conflicts of Interest: The authors declare no conflict of interest.

References

- Chen, S.; Gong, B. Response and adaptation of agriculture to climate change: Evidence from China. *J. Dev. Econ.* **2021**, *148*, 102557. [\[CrossRef\]](#)
- Qian, F.; Yang, J.; Torres, D. Comparison of corn production costs in China, the US and Brazil and its implications. *Agric. Sci. Technol.* **2016**, *17*, 731–736.
- Hou, L.; Wang, K.; Wang, Y.; Li, L.; Ming, B.; Xie, R.; Li, S. In-field harvest loss of mechanically-harvested maize grain and affecting factors in China. *Int. J. Agric. Biol. Eng.* **2021**, *14*, 29–37.
- Wang, K.; Xie, R.; Ming, B.; Hou, P.; Xue, J.; Li, S. Review of combine harvester losses for maize and influencing factors. *Int. J. Agric. Biol. Eng.* **2021**, *14*, 1–10.
- Fu, J.; Yuan, H.; Zhang, D.; Chen, Z.; Ren, L. Multi-Objective Optimization of Process Parameters of Longitudinal Axial Threshing Cylinder for Frozen Corn Using RSM and NSGA-II. *Appl. Sci.* **2020**, *10*, 1646. [\[CrossRef\]](#)
- Yang, L.; Cui, T.; Qu, Z.; Li, K.; Yin, X.; Han, D.; Yan, B.X.; Zhao, D.; Zhang, D. Development and application of mechanized maize harvesters. *Int. J. Agric. Biol. Eng.* **2016**, *9*, 15–28.
- Wang, L.; Yu, Y.; Ma, Y.; Feng, X.; Liu, T. Investigation of the Performance of Different Cleaning Devices in Maize Grain Harvesters Based on Field Tests. *Trans. ASABE* **2020**, *63*, 809–821. [\[CrossRef\]](#)
- Li, H.; Li, Y.; Gao, F.; Zhao, Z.; Xu, L. CFD–DEM simulation of material motion in air-and-screen cleaning device. *Comput. Electron. Agric.* **2012**, *88*, 111–119. [\[CrossRef\]](#)
- Badretdinov, I.; Mudarisov, S.; Lukmanov, R.; Permyakov, V.; Ibragimov, R.; Nasyrov, R. Mathematical modeling and research of the work of the grain combine harvester cleaning system. *Comput. Electron. Agric.* **2019**, *165*, 104966. [\[CrossRef\]](#)
- Ueka, Y.; Matsui, M.; Inoue, E.; Mori, K.; Okayasu, T.; Mitsuoka, M. Turbulent flow characteristics of the cleaning wind in combine harvester. *Eng. Agric. Environ. Food* **2012**, *5*, 102–106. [\[CrossRef\]](#)
- Gebrehiwot, M.G.; De Baerdemaeker, J.; Baelmans, M. Effect of a cross-flow opening on the performance of a centrifugal fan in a combine harvester: Computational and experimental study. *Biosyst. Eng.* **2010**, *105*, 247–256. [\[CrossRef\]](#)
- Wang, L.; Wu, Z.; Feng, X.; Li, R.; Yu, Y. Design and experiment of curved screen for maize grain harvester. *Trans. Chin. Soc. Agric. Mach.* **2019**, *50*, 90–101.
- Wang, L.; Feng, X.; Zheng, Z.; Yu, Y.; Liu, T.; Ma, Y. Design and test of combined sieve of maize screening. *Trans. Chin. Soc. Agric. Mach.* **2019**, *50*, 104–113.
- Sabashkin, V.A.; Sukhoparov, A.A.; Sinitsyn, V.A.; Zakharov, S.E. Removing straw impurities from grain heaps by cylindrical sieve. *Sib. Her. Agric. Sci.* **2017**, *47*, 80–87. [\[CrossRef\]](#)
- Ivanov, N.M.; Fedorenko, I.Y.; Zakharov, S.E.; Sukhoparov, A.A. Evaluating grain feed at separation by planetary cylindrical sieve with round holes. *Sib. Her. Agric. Sci.* **2017**, *47*, 72–79. [\[CrossRef\]](#)
- Krzysiak, Z.; Samociuk, W.; Zarajczyk, J.; Kaliniewicz, Z.; Pieniak, D.; Bogucki, M. Analysis of the sieve unit inclination angle in the cleaning process of oat grain in a rotary cleaning device. *Processes* **2020**, *8*, 346. [\[CrossRef\]](#)
- Cheng, C.; Fu, J.; Hao, F.; Chen, Z.; Zhou, D.; Ren, L. Effect of motion parameters of cleaning screen on corn cob blocking law. *J. Jilin Univ.* **2021**, *51*, 761–771.
- Xu, L.; Wei, C.; Liang, Z.; Chai, X.; Li, Y.; Liu, Q. Development of rapeseed cleaning loss monitoring system and experiments in a combine harvester. *Biosyst. Eng.* **2019**, *178*, 118–130. [\[CrossRef\]](#)
- Craessaerts, G.; Saeys, W.; Missotten, B.; De Baerdemaeker, J. A genetic input selection methodology for identification of the cleaning process on a combine harvester, Part I: Selection of relevant input variables for identification of the sieve losses. *Biosyst. Eng.* **2007**, *98*, 166–175. [\[CrossRef\]](#)
- Craessaerts, G.; de Baerdemaeker, J.; Missotten, B.; Saeys, W. Fuzzy control of the cleaning process on a combine harvester. *Biosyst. Eng.* **2010**, *106*, 103–111. [\[CrossRef\]](#)

21. Li, Y.; Xu, L.; Zhou, Y.; Li, B.; Liang, Z.; Li, Y. Effects of throughput and operating parameters on cleaning performance in air-and-screen cleaning unit: A computational and experimental study. *Comput. Electron. Agric.* **2018**, *152*, 141–148. [\[CrossRef\]](#)
22. Yuan, J.; Li, H.; Qi, X.; Hu, T.; Bai, M.; Wang, Y. Optimization of airflow cylinder sieve for threshed rice separation using CFD-DEM. *Eng. Appl. Comput. Fluid Mech.* **2020**, *14*, 871–881.
23. Wang, Z.; Liu, C.; Wu, J.; Jiang, H.; Zhao, Y. Impact of screening coals on screen surface and multi-index optimization for coal cleaning production. *J. Clean. Prod.* **2018**, *187*, 562–575. [\[CrossRef\]](#)
24. Zendehboudi, A.; Li, X. Desiccant-wheel optimization via response surface methodology and multi-objective genetic algorithm. *Energy Convers. Manag.* **2018**, *174*, 649–660. [\[CrossRef\]](#)
25. Sun, X.; Kim, S.; Yang, S.D.; Kim, H.S.; Yoon, J.Y. Multi-objective optimization of a Stairmand cyclone separator using response surface methodology and computational fluid dynamics. *Powder Technol.* **2017**, *320*, 51–65. [\[CrossRef\]](#)
26. Ren, L.Q. *Design of Experiment and Optimization*; Higher Education Press: Beijing, China, 2009; pp. 246–257.
27. Kim, I.; Ha, J.-H.; Jeong, Y. Optimization of Extraction conditions for antioxidant activity of acer tegmentosum using response surface methodology. *Appl. Sci.* **2021**, *11*, 1134. [\[CrossRef\]](#)
28. Babić, L.; Radojević, M.; Pavkov, I.; Babić, M.; Turan, J.; Zoranović, M.; Stanišić, S. Physical properties and compression loading behaviour of corn seed. *Int. Agrophys.* **2013**, *27*, 119–126. [\[CrossRef\]](#)
29. Selvam, T.A.; Manikantan, M.R.; Chand, T.; Sharma, R.; Seerangurayar, T. Compression loading behaviour of sunflower seeds and kernels. *Int. Agrophys.* **2014**, *28*, 543–548. [\[CrossRef\]](#)
30. Chen, Z.; Yu, J.; Xue, D.; Wang, Y.; Zhang, Q.; Ren, L. An approach to and validation of maize-seed-assembly modelling based on the discrete element method. *Powder Technol.* **2018**, *328*, 167–183. [\[CrossRef\]](#)
31. Castiglioni, C.A.; Drei, A.; Carydis, P.; Mouzakis, H. Experimental assessment of static friction between pallet and beams in racking systems. *J. Build. Eng.* **2016**, *6*, 203–214. [\[CrossRef\]](#)
32. González-Montellano, C.; Fuentes, J.M.; Ayuga-Téllez, E.; Ayuga, F. Determination of the mechanical properties of maize grains and olives required for use in DEM simulations. *J. Food Eng.* **2012**, *111*, 553–562. [\[CrossRef\]](#)
33. Wang, L.; Wu, B.; Wu, Z.; Li, R.; Feng, X. Experimental determination of the coefficient of restitution of particle-particle collision for frozen maize grains. *Powder Technol.* **2018**, *338*, 263–273. [\[CrossRef\]](#)
34. Sharma, R.K.; Bilanski, W.K. Coefficient of restitution of grains. *Trans. ASAE* **1971**, *14*, 216–218.
35. Cheng, C.; Fu, J.; Chen, Z.; Hao, F.; Cui, S.; Ren, L. Optimization experiment on cleaning device parameters of corn kernel harvester. *Trans. Chin. Soc. Agric. Mach.* **2019**, *50*, 151–158.
36. Park, C.I.L. Multi-objective optimization of the tooth surface in helical gears using design of experiment and the response surface method. *J. Mech. Sci. Technol.* **2010**, *24*, 823–829. [\[CrossRef\]](#)